Cancer Cell
Article

Adult Murine Prostate Basal and Luminal Cells Are Self-Sustained Lineages that Can Both Serve as Targets for Prostate Cancer Initiation

Nahyun Choi,[1,4] Boyu Zhang,[1,4] Li Zhang,[1] Michael Ittmann,[2,3] and Li Xin[1,2,3,*]
[1]Department of Molecular and Cellular Biology
[2]Department of Pathology and Immunology
[3]Dan L. Duncan Cancer Center
Baylor College of Medicine, One Baylor Plaza, Houston, TX 77030, USA
[4]These authors contributed equally to this work
*Correspondence: xin@bcm.edu
DOI 10.1016/j.ccr.2012.01.005

SUMMARY

The prostate epithelial lineage hierarchy and the cellular origin for prostate cancer remain inadequately defined. Using a lineage-tracing approach, we show that adult rodent prostate basal and luminal cells are independently self-sustained in vivo. Disrupting the tumor suppressor *Pten* in either lineage led to prostate cancer initiation. However, the cellular composition and onset dynamics of the resulting tumors are distinctive. Prostate luminal cells are more responsive to *Pten* null-induced mitogenic signaling. In contrast, basal cells are resistant to direct transformation. Instead, loss of Pten activity induces the capability of basal cells to differentiate into transformation-competent luminal cells. Our study suggests that deregulation of epithelial differentiation is a critical step for the initiation of prostate cancers of basal cell origin.

INTRODUCTION

Defining the cells of origin for cancer is of great value for accurate tumor prognosis and efficient prevention and therapeutics (Visvader, 2011). Previously, the identities of the cells of origin for cancer were assumed based on histological characterization of cancers. However, recent transcriptome studies have revealed that molecular signatures of cancer cells do not always match their histological appearance (Lim et al., 2009). Therefore, it can be misleading to determine cells of origin in the absence of functional lineage-tracing studies (Molyneux et al., 2010).

Though prostate cancer is the second leading cause of cancer-related death in males in the United States, it is still mainly described by qualitative clinical measurements, including the TNM system and the Gleason grading system (Iczkowski and Lucia, 2011). The identity of the cellular origin for prostate cancer remains unclear, partly because the prostate epithelial lineage hierarchy per se has not been clearly characterized. Prostate epithelia are composed of three types of epithelial cells, luminal cells, basal cells, and neuroendocrine cells, of which the latter are extremely rare (Abate-Shen and Shen, 2000). When prostate epithelial cells are cultured in vitro, a population of transit-amplifying cells is frequently observed (Litvinov et al., 2006; Peehl, 2005). These transit-amplifying cells express antigenic markers for both basal and luminal cells. Transit-amplifying cells are abundant at the developmental stage but are not detectable in vivo in adults under physiological conditions (Wang et al., 2001).

Using a functional prostate regeneration assay, several independent groups, including ours, have demonstrated that some basal cells in human and murine prostates can generate all three prostate epithelial cell lineages (Burger et al., 2005; Goldstein et al., 2010; Lawson et al., 2007; Leong et al.,

Significance

Understanding the cellular origin for cancer can help improve disease prevention and therapeutics. Our genetic studies directly demonstrate that prostate cancer can initiate from both the basal and luminal cell lineages. However, prostate basal cells are less susceptible than luminal cells to direct transformation. Instead, disease initiation from prostate basal cells requires oncogenic-signaling-induced differentiation of adult prostate basal cells into luminal cells, which is absent under physiological conditions. These studies suggest that deregulation of the normal-prostate epithelial differentiation program is a critical step for initiation of human prostate cancer with a basal cell origin. Furthermore, suppressing signaling pathways that induce basal-luminal differentiation may provide an efficient approach to prevent prostate cancer initiation.

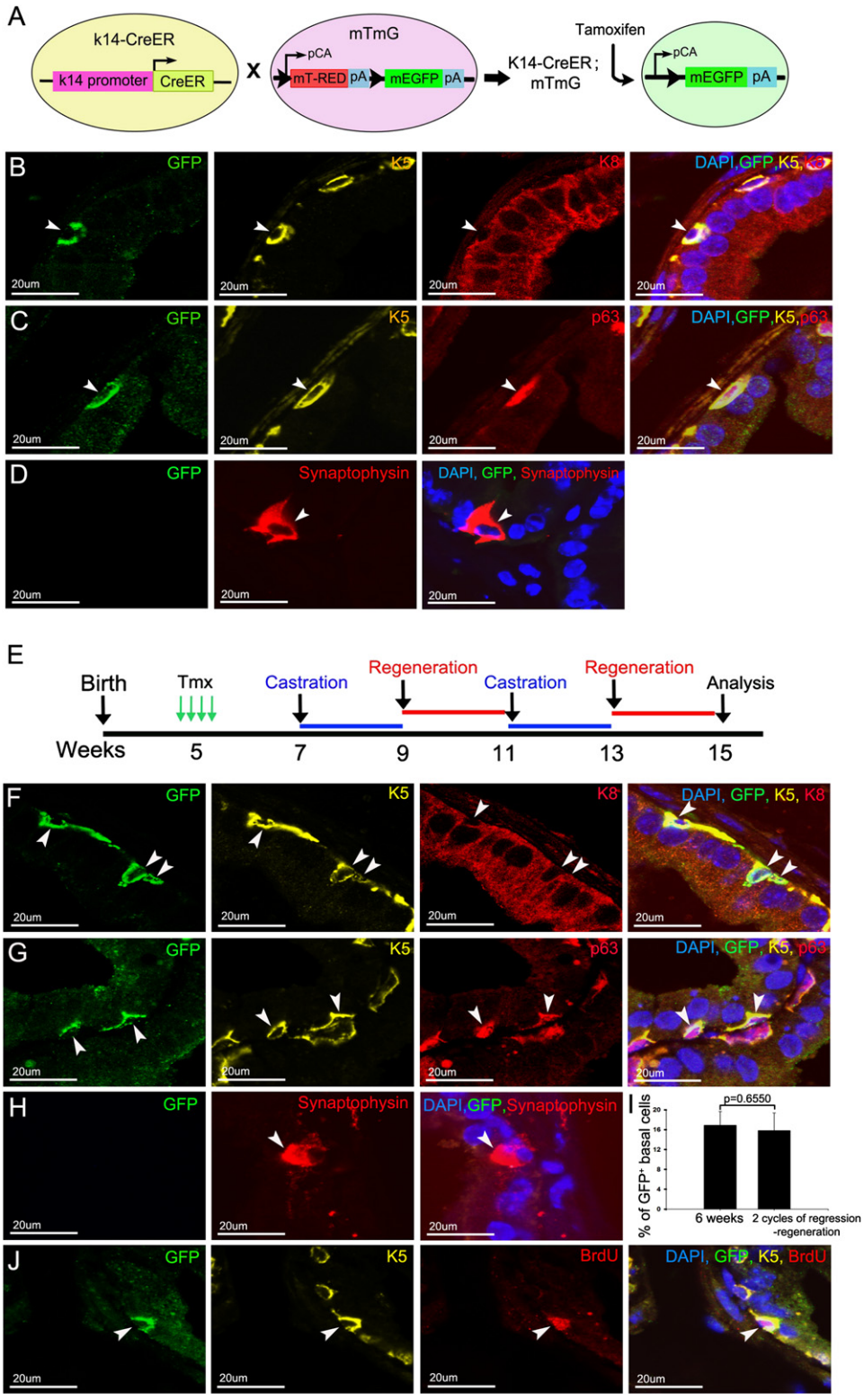

Figure 1. Lineage Tracing Shows that Prostate Basal Cells Only Generate Basal Cells In Vivo

(A) Schematic illustration of the lineage-tracing strategy.

(B–D) Costaining of GFP with K5 and K8 (B), K5 and P63 (C), and synaptophysin (D) in tamoxifen-treated K14-mTmG mice. Arrowheads in (B) and (C) indicate GFP-labeled basal cells. Arrowhead in (D) points to a neuroendocrine cell.

(E) Timeline for androgen deprivation and replacement experiments.

2008; Xin et al., 2005, 2007; Zhang et al., 2011). In addition, Wang et al. discovered that a rare castration-resistant luminal prostate cell population also possesses multipotent stem cell activity (Wang et al., 2009). Of note, the conclusions of those studies are based on experimental conditions involving cell transplantation that do not reflect physiological conditions. Therefore, it remains an open question whether the activities measured in those assays reflect the obligate or facultative function of prostate stem cells. Pertaining to this caveat, Liu et al. recently showed by lineage tracing that prostate luminal cells are derived from pre-existing luminal cells (Liu et al., 2011). In addition, a very recent comprehensive lineage-tracing study on the mammary gland epithelial lineage hierarchy showed that in the postnatal mammary gland, distinct stem cells contribute to the maintenance of the myoepithelial and luminal cell lineages (Van Keymeulen et al., 2011). A similar comprehensive study on prostate lineage hierarchy is required to address these controversies.

Previously, prostate luminal cells, transit-amplifying cells, and basal cells have all been implicated as the cells of origin for prostate cancer (Lawson and Witte, 2007). Two distinct functional approaches have been used recently to directly investigate the identity of the cellular origin for prostate cancer. One approach is to employ genetically engineered mouse models (Ellwood-Yen et al., 2003; Foster et al., 1997; Iwata et al., 2010; Majumder et al., 2003; Wang et al., 2003, 2009) to introduce oncogenic signaling in different prostate cell lineages. Most of these studies utilized two prostate-specific promoters (*Probasin* and *Nkx3.1*). However, recently it has been shown that these promoters are active in both luminal cells and some basal cells (Mulholland et al., 2009; Wu et al., 2007; Zhang et al., 2011). Therefore, one cannot determine definitively the identities of the cells of origin for cancer using this approach. Wang et al. recently demonstrated that some very rare NKX3.1-positive luminal cells in castrated mice can serve as targets for transformation (Wang et al., 2009), but it remains undetermined whether other luminal cells also can serve as the cells of origin for cancer. A prostate-specific antigen-CreER^{T2} model has recently been demonstrated to mediate luminal-cell-specific gene expression, but to date this model has not been extensively utilized (Liu et al., 2011; Ratnacaram et al., 2008).

The other approach is to genetically modify different prospectively isolated prostate epithelial cell lineages and investigate their tumorigenic potential by in vivo transplantation assays. Using this approach, we and others have demonstrated that murine and human prostate basal cells, but not luminal cells, can efficiently initiate prostate carcinogenesis in various oncogenic contexts (Goldstein et al., 2010; Lawson et al., 2010; Xin et al., 2005). However, a caveat for this approach is that luminal cells by nature do not proliferate and regenerate prostate tissues in the in vivo transplantation assay; hence, these studies cannot exclude that luminal cells also serve as the cells of origin for cancer in vivo. In summary, due to a lack of mouse models that enable strict lineage targeting in the prostate, it has not been comprehensively determined previously whether individual cell lineages can serve as targets for transformation orthotopically in the prostate. This study aims to reveal how prostate basal and luminal cell lineages are maintained and the roles of these two lineages in prostate cancer initiation.

RESULTS

Lineage Tracing Shows that Prostate Basal Cells Only Generate Basal Cells In Vivo

We employed a lineage-tracing approach to determine in vivo whether adult murine prostate basal epithelial cells would generate all three prostate epithelial cell lineages. A K14-CreER transgenic mouse line was generated previously (Vasioukhin et al., 1999) in which *CreER* is driven by the promoter of Keratin 14, a prostate basal cell marker. CreER encodes a Cre recombinase fused to a mutant estrogen ligand-binding domain so that its activity is induced only in the presence of tamoxifen. To investigate whether CreER is specifically expressed in prostate basal cells, K14-CreER transgenic mice were bred with *mTmG* reporter mice to generate K14-CreER$^{Tg/Tg}$;mTmG$^{Tg/Tg}$ mice (hereafter referred to as the K14-mTmG mice). The *mTmG* mouse line is a double fluorescent reporter line that replaces the expression of a membrane-targeted Tomato-Red (mT) protein with a membrane-targeted enhanced green fluorescence protein (mG) upon Cre-LoxP-mediated homologous recombination (Muzumdar et al., 2007) (Figure 1A).

Tamoxifen was injected intraperitoneally (i.p.) into male K14-mTmG bigenic mice. In contrast to the highly efficient Cre-mediated recombination observed in the skin (Figure S1A available online), the recombination efficiency in the prostate was lower and varied among different prostate lobes. On average, 17% of basal cells in lateral lobes were pulse-labeled with GFP (Table S1). In contrast, rare and heterogeneously distributed GFP-positive basal cells were observed in other lobes, and these cells were hard to quantify. The recombination frequencies among lobes did not correlate with the K14 promoter activity (Figure S1B). All GFP-positive cells expressed the basal cell marker keratin 5 (K5) (Figure 1B, Table S1; n = 2095 cells from five mice). All of the observed cell nuclei of these GFP-positive cells were positively stained with another nuclear-localized basal cell marker, P63 (Figure 1C; n = 1952 cells). In contrast, none of the examined GFP-positive cells expressed the luminal cell marker keratin 8 (K8), or the neuroendocrine cell marker synaptophysin (Figures 1B and 1D). These data demonstrate that the CreER expression is restricted to prostate basal cells in the K14-CreER model.

Adult murine prostate epithelia turn over extremely slowly under physiological conditions. To determine the fate of prostate basal cells, we induced extensive epithelial turnover by a classic

(F–H) Costaining of GFP with K5 and K8 (F), K5 and P63 (G), and synaptophysin (H) in tamoxifen-treated K14-mTmG mice after induced epithelial turnover. Arrowheads in (F) and (G) indicate GFP-labeled basal cells. Arrowhead in (H) points to a neuroendocrine cell.

(I) Bar graph shows the percentage of GFP-labeled basal cells in lateral prostate lobes of K14-mTmG mice 5 days after tamoxifen induction (6 weeks) and after 2 cycles of epithelial regression-regeneration. Data represent the mean ± SD. Also see Table S1.

(J) GFP-labeled basal cells (arrowhead) incorporated BrdU.

See also Figure S1 and Table S1.

prostate regression-regeneration model, as schematically illustrated in Figure 1E. In this model, prostate tissues atrophy and regenerate repeatedly in response to fluctuating serum testosterone levels. Substantial epithelial cell turnover was induced after two cycles of prostate regression-regeneration. Immunohistochemistry (IHC) analyses showed that all GFP-positive cells remained basal cells because they expressed K5 but not K8 or synaptophysin (n = 1295 cells from four mice, Figures 1F and 1H). In addition, the percentage of GFP-labeled basal cells in lateral prostates did not change after induced epithelial turnover (Figure 1I; Table S1), suggesting that either all basal cells possess equal regenerative capacity or the unipotent basal stem cells and differentiated basal cells are labeled at equal frequency. The GFP-labeled basal cells have proliferated because they incorporated BrdU (Figure 1J). Collectively, these data demonstrate that during prostate regeneration, the GFP-labeled basal cells proliferated but only gave rise to prostate basal cells and did not differentiate or undergo lineage conversion to generate other cell lineages.

Prostate Luminal Cell Lineage Is Self-Sustained In Vivo

We generated a K8-CreER^{T2} mouse model via bacterial artificial chromosome transgenesis (Zhang et al., 2012), in which CreER^{T2} is driven by the promoter of the prostate luminal cell marker keratin 8. The same lineage-tracing approach was employed using K8-CreERT2$^{Wt/Tg}$;mTmG$^{Wt/Tg}$ (hereafter referred to as K8-mTmG) mice to determine how prostate luminal epithelial cells are sustained. GFP was undetectable in vehicle-treated K8-mTmG mouse prostates (data not shown), but was expressed abundantly in tamoxifen-treated mouse prostates (Figure S2A). All GFP-positive cells expressed K8, but not K5 or synaptophysin [n = 31,319 from seven mice (Figures 2A and 2B)], demonstrating that CreER^{T2} is only expressed by prostate luminal epithelial cells in this model. The recombination efficiency varied among different prostate lobes, with that in lateral lobes the highest (Figures 2E and S2A; Tables S2 and S4). The recombination frequencies did not correlate with the K8 promoter activity (CreER expression level) among lobes (Figure S2B). Therefore, the variation in recombination efficiency may be due to differential local tamoxifen concentrations and CreER activation status as a result of distinct blood vessel densities among these different lobes.

To determine how the prostate luminal cell lineage is maintained, we aged tamoxifen-treated K8-mTmG mice for 4 months. As shown in Figure 2E and Tables S2–S4, the percentage of GFP-positive luminal cells in individual lobes did not change after aging. Since prostate tissues gain weight significantly from 6 weeks to 24 weeks (Figure S2C), it is unlikely that the invariant percentage of GFP-positive luminal cells after aging is due to rare cellular turnover. Instead, this result suggests that the luminal cell lineage may be self-sustained. To further interrogate this possibility, tamoxifen-treated K8-mTmG mice were subjected to two cycles of prostate regression-regeneration to induce extensive epithelial turnover, as illustrated in Figure 1E. IHC analyses showed that the percentages of GFP-positive luminal cells were not statistically different before and after induction of epithelial turnover (Figure 2E; Tables S2–S4). In addition, all GFP-positive cells still expressed K8, but not K5 or synaptophysin (Figures 2C and 2D), demonstrating that GFP-labeled luminal cells only generate other luminal cells. Overall these results imply that prostate luminal cells are not replenished by stem/progenitor cells from other cell lineages during prostate regeneration.

In addition, the approach illustrated in Figure 2F was employed to directly investigate the origin of newly formed prostate luminal cells. Tamoxifen-treated K8-mTmG mice were subjected to one cycle of prostate regression-regeneration to induce extensive epithelial turnover. BrdU was administered to label dividing cells during the period of regeneration. As shown in Figures 2G and 2H and Tables S2–S4, the GFP$^+$ new luminal cells (BrdU$^+$K8$^+$) in individual prostate lobes were generated at a frequency equal to that of the initial pulse-labeling (i.e., the percentage of GFP$^+$ luminal cells). These data suggest that if the labeling efficiency of luminal cells is 100%, all new K8$^+$ luminal cells will be GFP$^+$, which means that they would all come from cells in the luminal lineage existing at the time of castration and androgen replacement. In summary, these data directly demonstrate that the luminal cell lineage is self-sustained.

Prostate Cancer Initiated from Basal-Cell-Specific Loss of Function of PTEN

To determine the susceptibility of the prostate basal cell lineage to transformation induced by the loss of function of the tumor suppressor Pten, we generated K14-CreER$^{Tg/Tg}$;*Pten*$^{fl/fl}$ (K14-Pten) bigenic mice. Tamoxifen was administered to 5-week-old K14-Pten mice so that Pten was specifically disrupted in prostate basal cells. An ARR2PB-Cre;Pten$^{fl/fl}$ mouse model for prostate cancer was used as a control, in which Pten is disrupted in both basal and luminal cells (Wang et al., 2006; Zhang et al., 2011).

The disease progression status observed in all experimental mice is summarized in Table 1. Tamoxifen-treated K14-Pten mice displayed a shaggy fur phenotype (Figure S3A) with complete penetrance, as reported previously (Backman et al., 2004; Yao et al., 2006). Disrupting PTEN activity leads to phosphorylation of AKT that accumulates at the plasma membrane, which serves as a reliable marker for PTEN loss. AKT phosphorylation was uniformly detected in the epidermis (Figures S3B and S3C), demonstrating an efficient Pten knockout in the skin. As we showed previously, the activation of the CreER activity in K14-Pten mouse prostate basal cells was less efficient (Figure 1), but Pten was disrupted only in prostate basal cells, as demonstrated by costaining pAKT with P63 (Figures 3A–3A″). Pten deletion in prostate basal cells was further confirmed by PCR genotyping in in vitro cultured prostate spheres derived from basal cells in tamoxifen-treated K14-Pten mice (Mulholland et al., 2009) (Figure S3D). Surprisingly, no abnormal epithelial growth was noted in all the mice examined 1 month post tamoxifen treatment (Table 1). However, by 3 months post tamoxifen treatment, focal hyperplastic growth (Figure 3B) was observed in 4 out of 11 mice. Those prostatic intraepithelial neoplasia (PIN) lesions were graded from PIN1 to PIN4 using the nomenclature and criteria developed by Park et al. (2002). The PIN lesions, but not the adjacent normal tissues, expressed pAKT (Figure 3C). They contained both K5 positive basal cells and K8 positive luminal cells (Figures 3D and 3E). Luminal cells expanded in the PIN lesions as measured by the ratio of basal

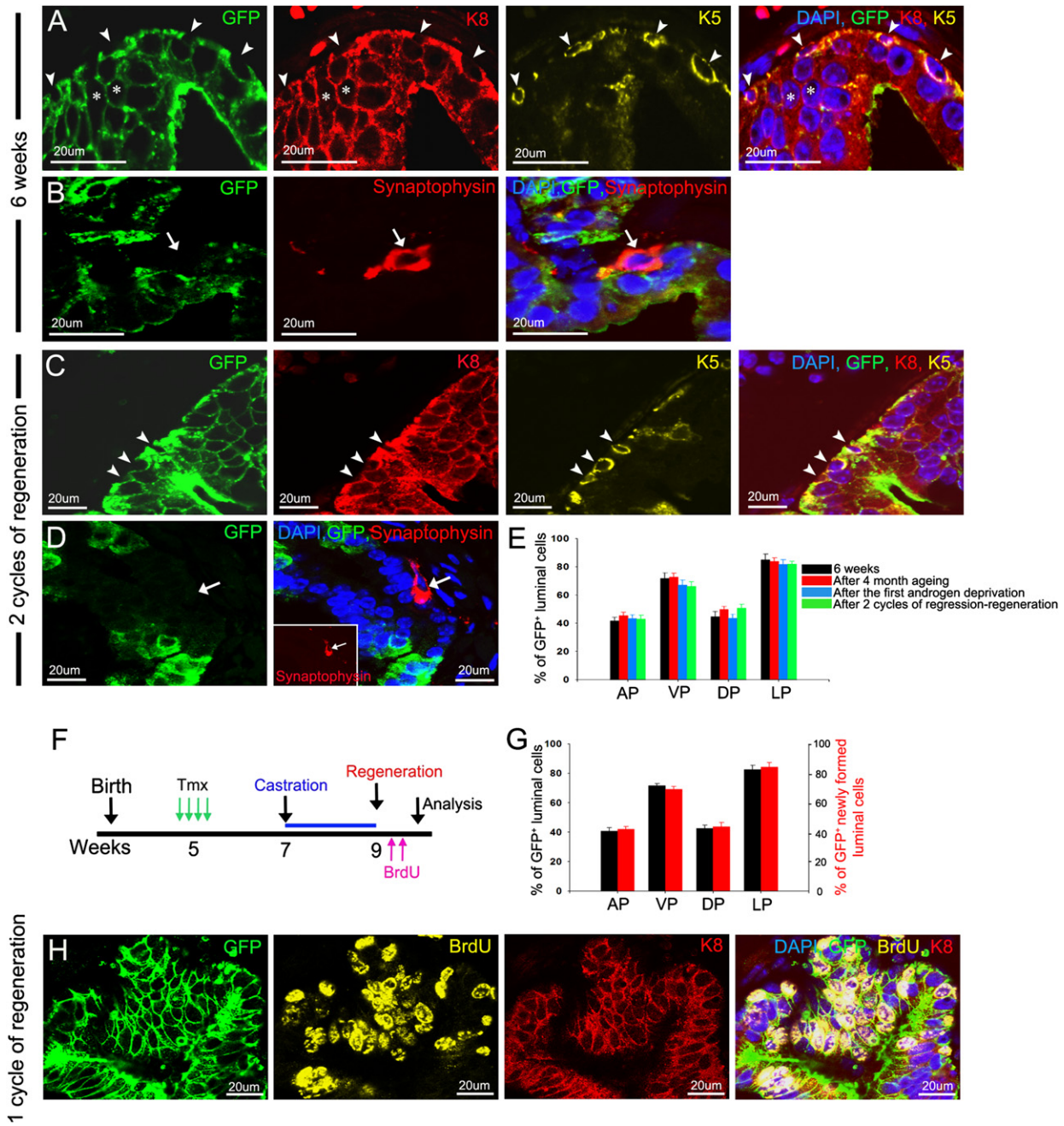

Figure 2. The Prostate Luminal Cell Lineage Is Self-Sustained In Vivo

(A and B) Costaining of GFP with K5 and K8 (A) and synaptophysin (B) in tamoxifen-treated K8-mTmG mice. Arrowheads and asterisks in (A) denote basal cells that are not GFP-labeled and GFP-labeled luminal cells, respectively. Arrow in (B) points to a neuroendocrine cell.

(C and D) Costaining of GFP with K5 and K8 (C) and synaptophysin (D) in tamoxifen-treated K8-mTmG mice after induced epithelial turnover. Arrowheads indicate that all basal cells are GFP negative. Arrow points to a neuroendocrine cell.

(E) Bar graph shows the percentage of GFP-labeled luminal cells 5 days after tamoxifen induction (6 weeks, black bars), after 4-month aging (red bars), after the first androgen deprivation (blue bars), and after two cycles of androgen deprivation-replacement experiments (green bars) in anterior (AP), ventral (VP), dorsal (DP), and lateral (LP) prostate lobes. Data represent the mean ± SD. See Tables S2–S4 for more details.

(F) Timeline for investigating the origin of newly formed luminal cells by BrdU labeling.

(G) Bar graph shows that the frequency of newly formed GFP-positive luminal ($GFP^+K8^+BrdU^+/K8^+BrdU^+$) cells reflects that of GFP-labeled luminal ($GFP^+K8^+/K8^+$) cells in all four prostate lobes. Data represent the mean ± SD. Also see Tables S2–S4.

(H) A representative image showing BrdU incorporated into luminal cells during prostate regeneration.

See also Figure S2 and Tables S2–S4.

Table 1. Summary of Disease Progression in K14-Pten and K8-Pten Mice

Month(s) Post Tmx Treatment	Tumor Incidence	Disease Stage/ Numbers of Mice	Mouse ID
K14-PTEN			
1	0/5	Normal/5	321,322,323,324,411
3	4/11	Normal/6	293,504,505,509,544
		PIN1/1	295
		PIN2/1	294
		PIN3/1	55
4		Normal/1	92
		PIN4/1	91
6	29/31	Normal/2	711,713
		PIN2/2	58,59
		PIN3/2	52,712
		PIN4/4	51,53,56,112
		Early cancer/2	57,111
7		PIN3/1	50
		PIN4/9	47,48,49,93,94, 95,98,456,460
8		PIN2/1	105
		PIN3/2	100,102
		PIN4/5	99,103,104,106,865
		Early cancer/1	101
K8-PTEN			
1	3/3	PIN1/1	89
		PIN2/1	69
		PIN3/1	146
2	9/9	Early cancer/2	159,924
3		PIN4/3	86,87,773
		Early cancer/3	89,772,774
4		Early cancer/1	307
6	15/15	PIN4/1	374
		Early cancer/12	226,229,237,375, 451,454,455,498, 499,503,876,898
		Adenocarcinoma/2	456,903

Disease stage is defined by the most advanced foci observed in tissues, most of which are within dorsolateral lobes.

versus luminal cells in epithelia (Figure 3F). Figures 3G and 3H show clearly that pAKT was also expressed in some basal cells, further corroborating that Pten deletion has taken place in those basal cells.

Six to eight months post tamoxifen induction, 29 out of 31 mice developed neoplastic foci at various stages (Table 1). Figures 4A and 4A′ shows images of K14-Pten mouse prostate glands 8 months after tamoxifen or vehicle treatment. The prostate lobes appeared less transparent in tamoxifen-treated mice. H&E staining revealed multifocal lesions that developed in all four lobes in this mouse (Figures 4B–4E). A majority of mice developed focal PIN4 and a few mice developed early prostate cancer, most frequently in the dorsolateral prostate (DLP). In most cases, the lumen of a few DLP lobes in individual mice was filled with epithelial cells with nuclear pleomorphism and hyperchromasia displaying tufting and cribriform patterns. The K14-Pten cancers were mainly composed of cells that were either positive for K5 or K8 (Figures 4F and 4H), with a small percentage of cells dual positive for K5 and K8. These double-positive cells express pAKT, suggesting they were also derived from Pten null basal cells (Figures S4A–S4C). In contrast, there were many $K5^{+}K8^{+}$ cells within the ARR2PB-Pten tumors (Figures 4G and 4H). Most of the K5 positive cells in K14-Pten mice were also positive for P63 (Figures 4I and 4J). Cells within the cancerous foci of K14-Pten mice express the androgen receptor and display secretory function, as demonstrated by the immunostaining of the secretory proteins of murine dorsolateral lobes (mDLP) (Donjacour et al., 1990) (Figures S4D–S4G). Finally, very few cells in K14-Pten tumors expressed the neuroendocrine cell marker synaptophysin (Figure 4K).

Sporadic basal cells that express pAKT were observed in glandular structures displaying normal histology (Figure 4L), suggesting that ablating *Pten* in basal cells is not sufficient to initiate prostate cancer. In contrast, cancer only initiated upon the emergence of pAKT-expressing luminal cells, thus suggesting that transition of basal cells into luminal cells may be both essential and a limiting step for cancer initiation in this model. We found that disease progression dynamics among experimental mice varied, with some developing into PIN4 to early cancer; while others remained as PIN2/3 even 6–8 months post tamoxifen induction (Figure 4M–4O). This is probably because the transition from basal cells to luminal cells occurred with different kinetics in those mice. Overall, our study suggests that loss of function of PTEN induces differentiation of prostate basal cells into luminal cells, which is an essential step for disease initiation in this model.

To investigate whether K14-Pten tumor cells have functional repopulating activity, we enzymatically dissociated primary tumors into single cells, mixed them with embryonic urogenital sinus mesenchymal cells, and transplanted them subcutaneously into immunodeficient host mice for 2 months, as done previously using the PB-Pten mouse model (Mulholland et al., 2009). Figure 4Q showed that K14-Pten tumor cells were capable of regenerating hyperplastic prostate glandular structures. Those glands were composed of basal cells and luminal cells that both expressed activated pAKT (Figures 4P–4S), further confirming that they were Pten null.

Prostate Cancer Derived from Luminal-Cell-Specific Loss of Function of PTEN

K8-CreERT2$^{Tg/wt}$;*Pten*$^{fl/fl}$ (K8-Pten) mice were generated to determine whether prostate cancer initiates as a result of luminal-cell-specific loss of function of *Pten* (Table 1). K8-Pten mice developed low-grade PIN lesions in all lobes at full penetrance 1 month post tamoxifen treatment (Figures 5A–5A″). There were fewer pAKT-expressing cells in the anterior prostate (AP) (data not shown), suggesting that the homologous recombination is less efficient in the AP. We showed that even when Pten disruption was induced in very few luminal cells using a lower dosage of tamoxifen, hyperplastic foci still formed 1 month post tamoxifen induction (Figures S5A–S5G). This suggests that the more rapid disease progression in the K8-Pten model, compared with the K14-Pten model, is due to the intrinsic differential response of these two cell lineages to Pten ablation, but is

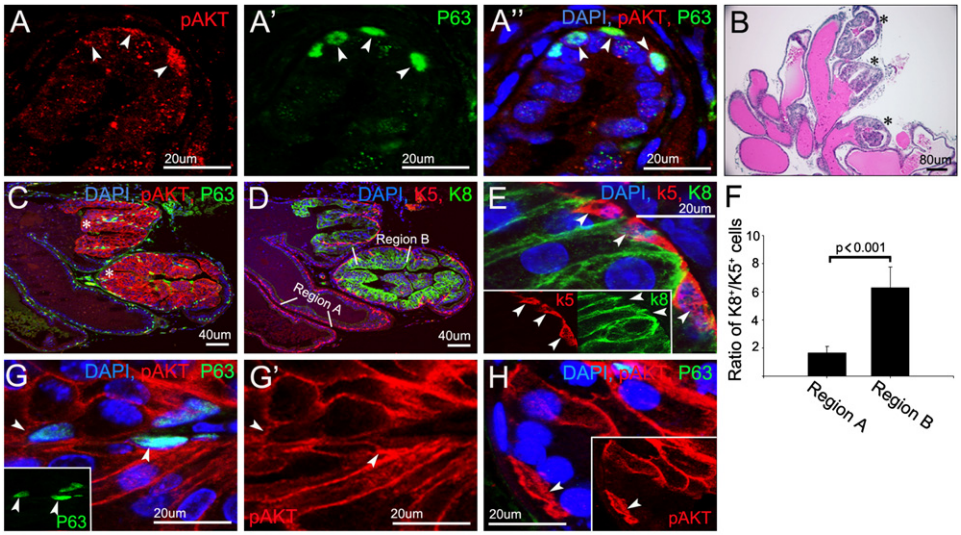

Figure 3. Prostate Cancer Initiated from Basal Cell-Specific Loss of Function of PTEN

(A-A″) Costaining of basal cell marker P63 (A′, A″) with pAKT (A, A″) in K14-Pten mice 1 month post tamoxifen induction. Arrowheads point to $pAKT^{+}P63^{+}$ cells.

(B) H&E staining of a K14-Pten prostate 3 months post tamoxifen induction reveals the formation of PIN lesions (asterisks).

(C) PIN lesions (asterisks), but not adjacent normal glands, express pAKT.

(D and E) PIN lesions contain both K5-expressing basal cells and K8-expressing luminal cells. Arrowheads indicate K5-expressing basal cells that encapsulate glands.

(F) Quantification of the expansion of luminal cells in PIN lesions (region B) as compared in normal glands (region A). Data represent the mean ± SD.

(G and H) Pten is disrupted in some basal cells. Arrowheads in (G) and (G′) denote a P63-expressing basal cell that expresses pAKT. Arrowhead in (H) points to an anatomically typical basal cell that expresses pAKT.

See also Figure S3.

not likely because that Pten deletion was induced in more cells in the K8-Pten model. The prostate hyperplasia progressed to PIN4 or early cancers 2–4 months post treatment (Figures 5B–5B″). Mitotic figures and large atypical cells with enlarged nuclei, prominent nucleoli, and hyperchromasia were observed. Early cancer or even frank adenocarcinoma formed unanimously 6 months post tamoxifen induction (Figures 5C–5C″). More than 95% of the glands in DLP and ventral prostate (VP) displayed a tufting and cribriform growth pattern, while the APs were more histologically heterogeneous, consisting of both normal and cancerous glands. This is probably due to the relatively lower frequency of homologous recombination in AP, as mentioned above.

The PIN lesions in ventral prostates were composed predominantly of K8 positive luminal cells, while K5-or P63-positive basal cells were almost completely lost (Figure 5D). In comparison, in the AP and DLP, there was a dramatic expansion of the cells that were dual positive for K5 and K8 (Figures 5E and 5F), similar to the double-positive cells observed in the ARR2PB-Pten model (Figure 4G). The K5 staining in these dual-positive cells was cytoplasmic, in sharp contrast to the typical K5 staining in basal cells that highlights cellular contour. Since these double positive cells expressed activated AKT, they should have been derived from K8-positive luminal cells, presumably becoming putative transit-amplifying cells through dedifferentiation (Figures 5H and 5I) (Litvinov et al., 2006). They did not express P63 (Figures 5G–5I). In contrast, P63 was only expressed by the K5-positive basal cells residing at the basement membrane and did not express activated AKT (Figures 5J–5L), suggesting that these P63-expressing cells were bona fide basal cells that did not undergo homologous recombination. The differential phenotypes among lobes were observed consistently during the 6 months post tamoxifen treatment. Cancer cells in all lobes express the androgen receptor and mDLP, while synaptophysin-expressing neuroendocrine cells were very rare in all lobes (Figures S5H–S5N). The same observations were made when both Pten and P53 were knocked out in luminal cells using $K8\text{-}CreERT2^{Tg/Wt}$; $Pten^{fl/fl}$;$P53^{fl/fl}$ (K8-Pten;P53) mice (data not shown).

Transplantation assays again were performed to determine whether K8-Pten tumor cells were capable of functional repopulation. H&E staining shows that the outgrowth tissues contained both normal glandular structures and cancerous lesions (Figures 5M–5O). The normal prostate glandular structures were composed of a single layer of epithelial cells encircling lumen filled with eosinophilic secretions. Both prostate basal and luminal cells were detected in those glands (Figure 5P). They did not express pAKT (data not shown). We previously showed that only prostate basal cells are capable of forming such prostate glandular structures upon transplantation (Lawson et al., 2007; Xin et al., 2005). These results suggest that those normal glands were derived from prostate basal cells and further corroborate that Pten was not disrupted in prostate basal cells in the K8-Pten model. In contrast, the focal cancerous lesions were composed of cells that were double-positive for K5 and K8 and expressed pAKT (Figures 5Q and 5R). They did not express P63 (data not shown). This phenotype recapitulates that of the original tumors in the AP and DLP, suggesting that those lesions were derived from Pten-null luminal cells. Collectively, these

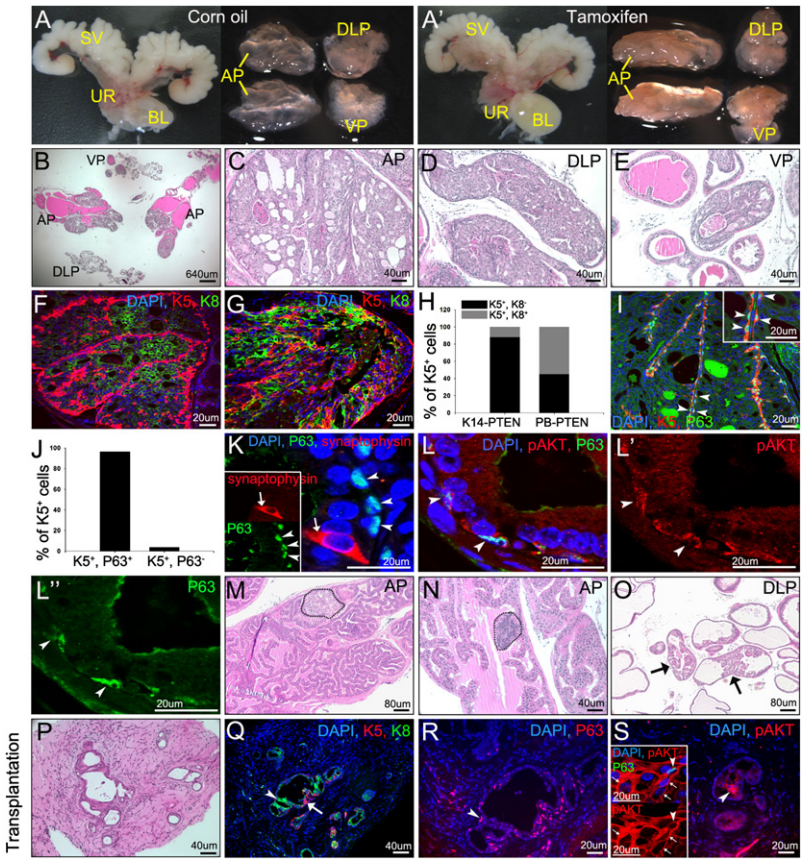

Figure 4. Progression of Prostate Cancer in the K14-Pten Model

(A and A′) Representative images of urogenital organs and dissected prostate lobes from K14-Pten mice 8 months after induction with vehicle (A′) or tamoxifen (A).

(B–E) Representative images of H&E staining of total prostate (B), AP (C), DLP (D), and VP (E) lobes of a K14-Pten mouse 8 months after tamoxifen treatment.

(F–H) Immunostaining of K5 and K8 of a K14-Pten mouse 3 months after tamoxifen treatment (F) and a 4-month old ARR2PB-Pten mouse (G). (H) Quantification of the percentage of $K5^+K8^+$ and $K5^+K8^-$ cells in the two models.

(I and J) Immunostaining of K5 and P63 in K14-Pten mice (I) and quantification of the percentage of $K5^+P63^+$ and $K5^+P63^-$ cells (J).

(K) Synaptophysin-expressing neuroendocrine cells (arrow) are rare in K14-Pten prostate tumor. Arrowheads point to P63-expressing basal cells.

(L–L″) Prostate basal cells in normal glands in tamoxifen-treated K14-Pten mice express pAKT. Arrowheads point to P63-expressing basal cells that express pAKT.

(M–O) Representative images of H&E staining show that only mild focal PIN lesions (dot-circled and arrow-pointed regions) are developed in many K14-Pten mice 6–8 months post tamoxifen treatment.

(P–S) Dissociated prostate cells from K14-Pten tumors are capable of regenerating abnormal glandular structures. (P) H&E staining of the outgrown tissues. (Q–S) Immunostaining of K5 (Q, arrow) and K8 (Q, arrowhead), P63 (R, arrowhead), and pAKT (S, arrowhead). Insets in (S) indicate that both basal (arrowhead) and luminal (arrow) cells express pAKT.

See also Figure S4.

data further support that disruption of Pten in prostate luminal cells causes prostate cancer.

Castration-Resistant Prostate Cancer Cells Exist in K8-Pten Prostate Tumors

To investigate the response of K8-Pten tumors to androgen deprivation, we castrated K8-Pten mice 4 months after tamoxifen induction. Seminal vesicles and prostate tumors shrunk significantly after androgen ablation (Figure 6A and 6A′), which demonstrated successful androgen ablation and corroborated that many cancer cells were dependent on androgen for their survival. Histological analysis confirmed substantial cell death in the prostate 10 days and 2 months postcastration, as evidenced by significant apoptotic bodies inside tumor masses and cellular debris inside prostate lumen (Figures 6B–6D). IHC analysis showed that two months postcastration the remaining VP tumors were composed predominantly of luminal cells (Figure 6E). The K5 and K8 double-positive cells decreased significantly but still persisted in the AP and DLP tumors (Figures 6F and 6G). These data demonstrate that these luminal cells survive androgen deprivation and suggest that they may serve as the cellular origin for castration-resistant prostate cancer.

Prostate Basal Cells Are Resistant to Direct Oncogenic Transformation

The above studies showed that prostate basal cells were less sensitive than luminal cells to mitogenic signals mediated by Pten deletion. We wondered whether this was due to the insufficient oncogenic potency conferred by *Pten* loss or to the indolent nature of basal cells to transformation. P53-dependent PTEN-deletion-induced cellular senescence has been shown to impede the rapid progression of fully developed prostate adenocarcinoma in the Pten-null prostate cancer model (Alimonti et al., 2010; Chen et al., 2005). We generated K14-CreER$^{Tg/Tg}$;*Pten*$^{fl/fl}$;*P53*$^{fl/fl}$ (K14-Pten;P53) mice and sought to determine whether prostate basal cells can be directly transformed upon simultaneous deletion of Pten and P53. Two months post tamoxifen induction, experimental mice developed severe hyperplastic growth in facial skin, showed signs of morbidity such as loss of weight and hunched postures, and had to be euthanized (Figures S6A–S6D). Seminal vesicles and prostates from tamoxifen-treated K14-Pten;P53 mice were much smaller compared to the control mice, probably due to morbidity (Figure S6E). H&E staining showed that prostate epithelial cells packed tightly due to reduced cytoplasmic volumes. There were no signs of hyperproliferation (Figures 7A and 7B; N = 9 mice), which was corroborated by a lack of Ki67-expressing cells (data not shown). The glandular structures were mostly composed of K5-positive basal cells that encapsulated K8-positive luminal cells (Figure 7C). Occasionally, basal cells were reduced in number in some glands (Figure 7D). IHC analyses showed clearly that pAKT was activated only in P63-expressing basal cells, demonstrating that Pten was only disrupted in basal cells (Figure 7E). PCR analysis confirmed that

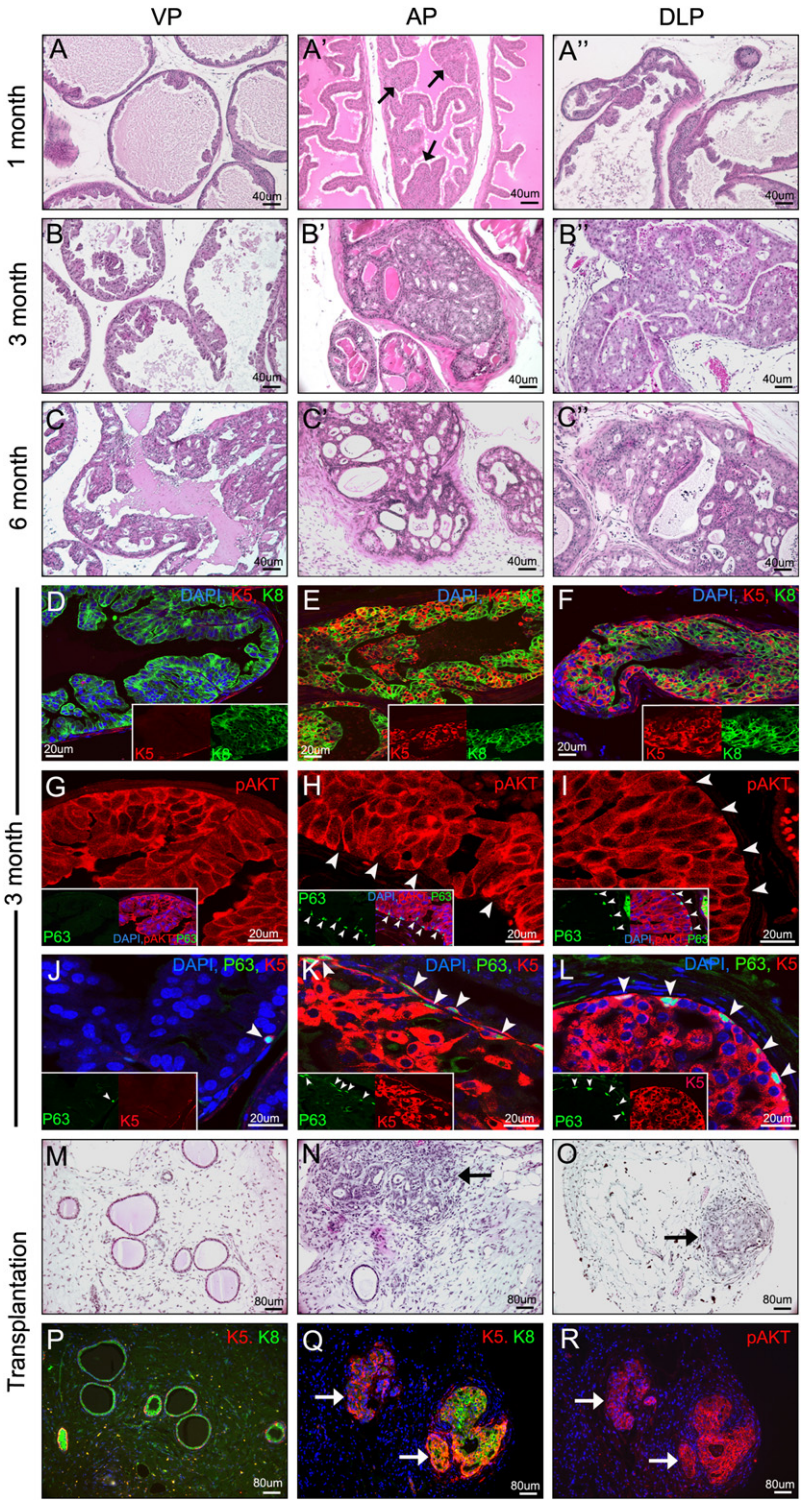

Figure 5. Prostate Cancer Derived from Luminal-Cell-Specific Disruption of PTEN

(A–C) H&E staining of AP (A′, B′, C′), VP (A, B, C), and DLP (A″, B″, C″) lobes of K8-Pten mice at 1, 3, and 6 months post tamoxifen induction. Arrows point to focal hyperplasia in AP.

(D–F) Immunostaining of K5 and K8 reveals a distinct lineage composition among VP (D), AP (E), and DLP (F).

(G–I) P63-expressing basal cells (arrowheads) do not express pAKT in VP (G), AP (H), and DLP (I).

(J–L) Only K5-expressing basal cells residing at the basement membrane express P63 (arrowheads) in VP (J), AP (K), and DLP (L).

(M–R) K8-Pten prostate tumor can repopulate. Representative images of H&E staining of outgrown tissues from dissociated K8-Pten tumor tissues (M–O). Immunostaining of K5 and K8 (P and Q), and pAKT (R) of outgrown tissues. Arrows indicate cancerous foci.

See also Figure S5.

successful ablation of *P53* (Figure S6F). We were able to keep four K14-Pten;P53 mice for 3 months after tamoxifen treatment and observed one PIN4 lesion in one mouse (Figure 7F, arrow), which demonstrates that cancer can initiate from basal cells with *Pten* and *P53* deletion. The PIN4 lesion is mainly composed of luminal cells expressing K8, with some cells expressing K5 only or both K5 and K8 (Figure 7G). Some P63-expressing basal cells expressed pAKT, suggesting that *Pten* was disrupted in those cells (Figure 7H). To exclude that the morbidity of experimental mice interferes with disease progression in the prostate, we collected intact prostate lobes from K14-Pten;P53 mice 2 months post tamoxifen treatment and transplanted them under the kidney capsules of immunodeficient male hosts. Only a few PIN1 lesions were noted in 7-week transplants (Figures 7I–7K). In contrast, massive lesions at the PIN4 or early cancer stages were observed in 15-week transplants (Figures 7L–7N). Within those cancerous regions, some P63-expressing basal cells express pAKT while other do not, suggesting that Pten was disrupted in only a fraction of basal cells (Figures 7O–7P). Collectively, these results imply that basal cells in situ are by nature relatively resistant to direct transformation by oncogenic stimuli, which partly explains why prostate basal cell carcinoma is so rare (Ali and Epstein, 2007).

DISCUSSION

Obligate versus Facultative Stem Cell Capacity of the Prostate Basal Cells

Our study demonstrates that adult murine prostate basal and luminal cell lineages are independently sustained. We and others also showed previously, using a transplantation-based prostate regeneration assay, that some prostate basal cells in both humans and rodents are capable of generating all three prostate epithelial cell lineages (Burger et al., 2005; Goldstein et al., 2010; Lawson et al., 2007; Leong et al., 2008; Xin et al., 2005; Zhang et al., 2011). These two observations are not mutually contradictory since they may illustrate the obligate versus facultative activities of stem cells in the prostate basal cell lineage. In the prostate

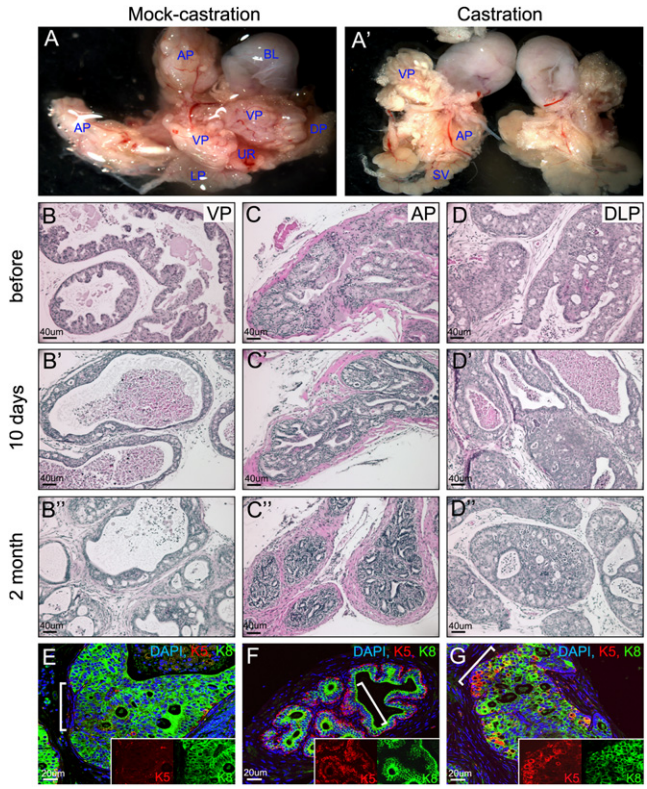

Figure 6. Castration-Resistant Prostate Cancer Cells Exist in K8-Pten Prostate Tumors

(A and A′) Representative images of urogenital organs excluding seminal vesicles from K8-Pten mice 2 months after a mock surgery (A) and castration (A′). BL, bladder; UR, Urethra; AP, anterior prostate; VP, ventral prostate; DP, dorsal prostate; LP, lateral prostate.

(B–G) H&E staining (B–D) and immunostaining of K5 and K8 (E–G) of VP (B and E), AP (C and F), and DLP (D and G) of K8-Pten mice before castration (B–D), and 10 days (B′–D′) and 2 months (B″–D″) after castration. Insets in (E)–(G) show staining of K5 and K8 at bracketed regions in respective images.

regeneration assay, basal cells are dissociated into single cells, removed from their natural environmental cues, and cocultured with embryonic urogenital sinus mesenchyme (UGSM) cells (Xin et al., 2003). It has been shown that embryonic stromal cells provide inductive signals that are absent in adult murine stromal cells, which affects epithelial cell differentiation or even changes their lineage status (Neubauer et al., 1983; Taylor et al., 2006). On the other hand, stromal-epithelial and epithelial-epithelial interactions in adult mouse prostate may mediate signaling that prevents basal cells from differentiating into other lineages. Our observations from the K14-mTmG and K14-Pten models demonstrate that oncogenic signals like *Pten* loss can alter the differentiation program of basal cells. In conclusion, we demonstrated that at least some prostate basal cells possess unipotent stem cell activity to maintain this lineage during prostate homeostasis and regeneration. In contrast, the results obtained using the prostate regeneration assay revealed the plasticity of the basal cell lineage in response to changes in environmental cues.

Of note, since only up to 21% of prostate basal cells were labeled with GFP in the K14-mTmG model, we cannot exclude the possibility that some of unlabeled basal cells can generate luminal cells and neuroendocrine cells. However, our complementary lineage tracing experiment using the K8-mTmG model suggests that the luminal cell lineage is mainly self-sustained. Therefore, even if these additional multipotent basal cells exist, differentiation of basal cells into luminal cells most likely would be rare during prostate regeneration. Recently, similar conclusions have been made in the mammary gland (Van Keymeulen et al., 2011). Though the mammary gland myoepithelial cells are capable of regenerating the mammary gland in vivo in transplantation assays, genetic lineage-tracing experiments demonstrated that the myoepithelial and luminal cell lineages are independently maintained in adults.

Maintenance of the Luminal Cell Lineage

Previously, a population of castration-resistant NKX3.1-expressing (CARN) luminal cells was shown to be able to generate all three prostate epithelial lineages (Wang et al., 2009). However, we did not observe in the K8-mTmG mice any descendant of GFP-positive luminal cells that expressed K5 or synaptophysin, suggesting that GFP-labeled luminal cells do not differentiate or convert into the other two epithelial cell lineages, at least in this mouse model. Since not all prostate luminal cells were labeled with GFP in the K8-mTmG model, we cannot exclude the possibility that CARN cells were preferentially not labeled under our experimental conditions.

Several lines of evidence imply the existence of a lineage hierarchy within the luminal cell lineage. Luminal cells are heterogeneous with regard to their capacity to retain BrdU labeling (Tsujimura et al., 2002). The androgen receptor expression level and activation status are heterogeneous among adult murine luminal cells (L.X., unpublished data). In addition, some luminal cells can survive androgen deprivation for an extended period (Tsujimura et al., 2002). It has been suspected that those androgen-independent luminal cells represent the committed progenitor cells in the luminal lineage. Our results showed that the percentage of GFP-positive luminal cells in castrated mice was approximately the same as that in intact mice (Figure 2E), which suggests that differentiated androgen-dependent luminal cells and androgen-independent luminal progenitor cells were GFP-labeled at a similar frequency. To date, the identity of the putative "luminal progenitor cells" remains undefined.

Alternatively, the androgen-independent survival of prostate luminal cells may be accounted for by a stochastic model in which any luminal cells could be conferred with the capacity for castration resistance when they happen to reside in a specific niche, such as a specialized anatomical location or a direct contact with a certain subtype of basal cells. In this scenario, the luminal cell lineage may be sustained simply by cell duplication, like the β cells in the pancreas (Dor et al., 2004). Future effort should be made to distinguish the two models.

Prostate Basal Cells as the Cellular Origin for Prostate Cancer

Our studies demonstrated that although both prostate basal and luminal cells can serve as the cellular origin for prostate cancer, prostate luminal cells are more sensitive to mitogenic signaling, while basal cells are relatively resistant to transformation. This is consistent with the fact that luminal cells

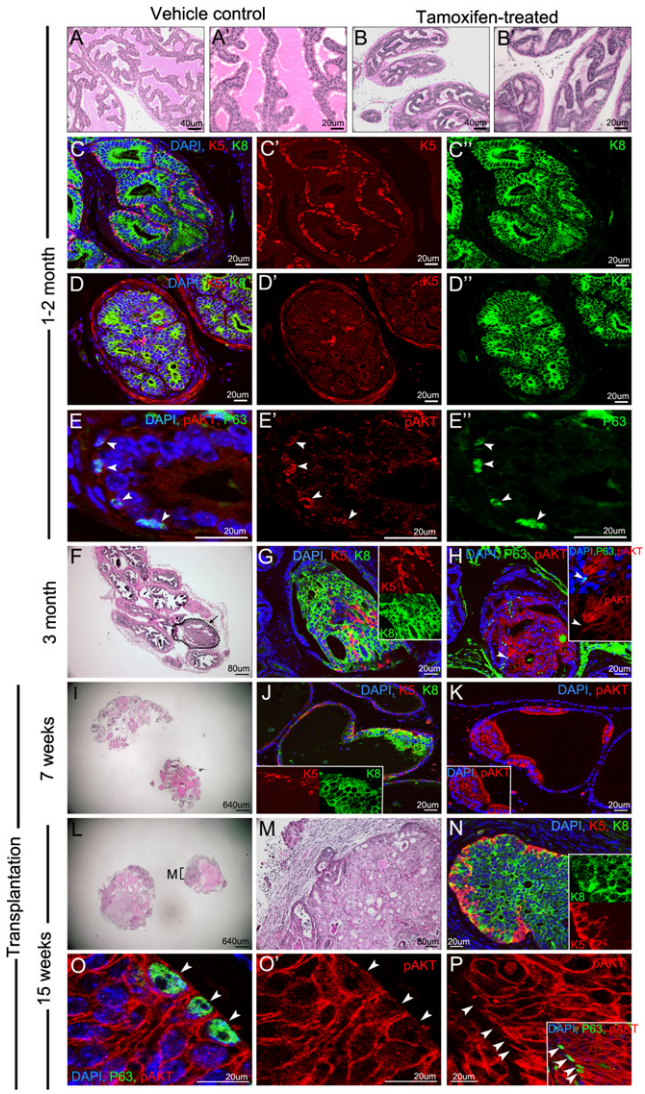

Figure 7. Prostate Basal Cells Are Resistant to Direct Oncogenic Transformation

(A and B) H&E staining of K14-Pten;P53 mouse prostates 2 months after vehicle (A) or tamoxifen (B) induction. A′ and B′ show images of higher magnification.

(C and D) Representative images of immunostaining of K5 and K8 of prostates from K14-Pten;P53 mice 2 months post tamoxifen induction.

(E) Pten is disrupted only in basal cells in K14-Pten;P53 mice, as demonstrated by costaining of pAKT (E and E′) and P63 (E and E″). Arrowheads indicate pAKT-expressing cells that also express P63.

(F–H) H&E (F) and immunostaining of K5/K8 (G) and pAKT/P63 (H) of K14-Pten;P53 mouse prostates 3 months after tamoxifen induction. Arrow in F points to a dot-circled PIN4 lesion. Arrowhead in H points to a basal cell expressing pAKT.

(I–P) Two months after tamoxifen treatment, K14-Pten;P53 prostate glands were transplanted under renal capsules of immunodeficient male hosts. H&E staining (I, L, and M) and immunostaining of K5/K8 (J and N) and pAKT/P63 (K, O, and P) of 7-week (I–K) and 15-week (L–P) transplants. Arrowheads in O and P denote P63-expressing cells that express and do not express pAKT, respectively.

See also Figure S6.

possess low levels of H2A.X and hence are more vulnerable to oncogenic stress (Jäämaa et al., 2010). The distinctive responses of these two cell lineages to oncogenic insults explain why treatment-naive prostate cancers are mostly composed of luminal cells, while prostate basal cell carcinoma is very rare.

Intuitively, prostate basal cells would seem to be the preferred cellular origin for cancer because they are more prone to accumulating genetic alterations than luminal cells. They are less well differentiated and proliferate more frequently (Bonkhoff et al., 1994). Additionally, they are proposed to act as a natural barrier to protect the luminal cell lineage from various insults. Thus, they are exposed to a more "hostile" environment than are luminal cells. For example, the basal cells are in closer contact with various cancer-promoting cytokines generated by the surrounding reactive stroma as a result of chronic inflammation (Tuxhorn et al., 2001). However, since most prostate cancers display a luminal cell phenotype, differentiation of basal cells into luminal cells becomes an essential and probably a rate-limiting step for cancer initiation and progression, if the cellular origin for cancer is of the basal cell lineage. This is supported by our result from the K14-Pten model. Prostate cancer was initiated in the K14-Pten model with an increased latency. Though Pten was disrupted specifically only in the prostate basal cells, the initiation of cancer did not start until the emergence of pAKT-expressing luminal cells. Since direct differentiation of basal cells to luminal cells is absent under physiological conditions based on our lineage-tracing experiments, these results suggest that deregulation of the normal prostate epithelial differentiation program is a critical step for initiation of human prostate cancer with a basal cell origin.

It should be noted that the most ideal way to investigate the cells of origin for cancer is to perform lineage tracing in the cancer models. However, we were not able to perform our study in this way for two reasons. First, activation of CreER^{T2} by tamoxifen is transient. Therefore, homologous recombination may not be achieved in all the cells that express CreER^{T2}, as we have shown in the K14-mTmG and K8-mTmG lineage-tracing experiments (Figures 1 and 2). Second, the recombination efficiencies at different genomic loci are not identical. As shown in Figures S5O and S5P, GFP expression does not guarantee Pten deletion in tamoxifen-treated K8-*Pten*$^{fl/fl}$-mTmG triple transgenic mice. Nevertheless, we found that the specificities of the K14 and K8 promoters are not affected by the genetic background of the experimental mice (Figures S5Q and S5R). In addition, we confirmed lineage specific *Pten* deletion by costaining pAKT with lineage markers in the K14-Pten and K8-Pten models. Therefore, we can conclude that neoplasia and tumors in the K14-Pten and K8-Pten models are derived from basal and luminal cells, respectively.

A unique feature of prostate cancer is that the disease is strictly age-dependent. Men under 35 seldom develop prostate cancer. Our data showed that it takes at least 3 months for K14-Pten mouse prostate basal cells to differentiate into luminal cells, which is almost equivalent to 10 years of human life, suggesting that this is still an extremely lengthy and inefficient biological process under certain genetic contexts. This may provide an additional explanation for the strict age-dependent nature of human prostate cancer.

Prostate Luminal Cells as the Cellular Origin for Primary and Castration-Resistant Prostate Cancer

Our genetic model also supports that luminal cells can be the cellular origin for prostate cancer. An intriguing observation from our K8-Pten model is that the same genetic change causes tumors with lobe-specific phenotypes with regard to their cellular composition. The phenotype in VP resembles that of the human disease because markers of basal cells are absent in prostate carcinoma, which has served as a diagnostic criterion for prostate cancer. In comparison, tumors in the AP and DLP are composed of cells that express both K5 and K8, and basal cells remain largely unaffected. A previous study has revealed a compartmentalization of gene expression between prostate lobes and identified dozens of differentially expressed genes between prostate lobes (Abbott et al., 2003). It is possible that the cellular context, i.e., the intrinsic differences in gene expression between prostate lobes, leads to the differential responses of the lobes to the oncogenic insult. It will be interesting to investigate whether human prostate luminal cells share more similarity with murine VP luminal cells in terms of gene expression profiles. The mechanism by which basal cells are depleted in the VP is also unknown. We recently reported that dissociation of basal cells leads to cellular apoptosis induced by activation of the RhoA/ROCK kinases (Zhang et al., 2011). One potential mechanism, therefore, could be that the basal cell layer in ventral prostate is less resilient to cellular perturbations, so that when prostate glands are enlarged and distorted due to excessive proliferation of prostate luminal cells, the cellular contact between ventral prostate basal cells is attenuated, which alters the signaling that regulates basal cell survival, such as the RhoA/ROCK-mediated signaling.

Our study also demonstrates that castration-resistant cells in prostate cancers may originate from luminal cells. This result excludes the possibility that prostate basal cells are the only cellular origin for castration-resistant disease. Since there is no evidence that CARN cells (Wang et al., 2009) were genetically manipulated by tamoxifen induction in the K8-CreER^{T2} model (Figure 2), our study also suggests that CARN cells are not the only cells of origin for prostate cancer in the luminal cell lineage, and that castration resistance is not a unique feature of CARN cells. This observation further highlights the need to identify the androgen-independent prostate luminal progenitor cells and to determine the essential signaling that confers the capacity for androgen-independent survival to luminal cells.

EXPERIMENTAL PROCEDURES

Mouse Procedures

The sources of experimental mice and the genotyping strategies are described in Supplemental Experimental Procedures. Castration, androgen replacement, dissociation of primary prostate tumors, and tumor cell transplantation were performed using standard techniques described in Supplemental Experimental Procedures. Tamoxifen (Sigma-Aldrich, St. Louis, MO) was dissolved into corn oil and was administrated i.p. into experimental mice at the age of 5 weeks once a day for four consecutive days. The dosages used for K14-CreER and K8-CreER^{T2} mice were 9 mg/40 g and 2 mg/40 g, respectively. All animal work were approved by and performed under the regulation of the Institutional Animal Care Committee of the Baylor College of Medicine.

Histology, Immunohistochemical, and Immunofluorescent Analysis

The procedures for histological and IHC analyses and the information about primary antibodies were described in Supplemental Experimental Procedures. Paraffin-embedded sections were stained and counterstained with 4,6-diamidino-2-phenylindole (DAPI) (Sigma-Aldrich, St. Louis, MO). Secondary antibodies were labeled with Alexa Fluro 488, 594, 633 (Invitrogen, Carlsbad, CA). Immunofluorescence staining was imaged using an Olympus BX60 fluorescence microscope or a Leica EL6000 confocal microscope. Cell counting was performed either manually or via ImagePro Software.

Statistics

All experiments were performed using 4–10 mice in independent experiments. Data are presented as mean ± SD. Student's t test was used to determine significance between groups. For all statistical tests, the 0.05 level of confidence was accepted for statistical significance.

SUPPLEMENTAL INFORMATION

Supplemental Information includes six figures, four tables, and Supplemental Experimental Procedures and can be found with this article online at doi:10.1016/j.ccr.2012.01.005.

ACKNOWLEDGMENTS

We thank Dr. Larry Donhower for the P53 conditional mice, Dr. Hong Wu for the Pten conditional mice, Dr. Gerald Cunha for antiserum against mDLP, Dr. Jeffrey Rosen for critical comments, Dr. Michael Lewis for sharing the NOD/SCID mouse colony. This work is supported by NIH R00CA125937, R01DK092202, and U01CA141497.

Received: October 28, 2011
Revised: January 2, 2012
Accepted: January 6, 2012
Published: February 13, 2012

REFERENCES

Abate-Shen, C., and Shen, M.M. (2000). Molecular genetics of prostate cancer. Genes Dev. *14*, 2410–2434.

Abbott, D.E., Pritchard, C., Clegg, N.J., Ferguson, C., Dumpit, R., Sikes, R.A., and Nelson, P.S. (2003). Expressed sequence tag profiling identifies developmental and anatomic partitioning of gene expression in the mouse prostate. Genome Biol. *4*, R79.

Ali, T.Z., and Epstein, J.I. (2007). Basal cell carcinoma of the prostate: a clinicopathologic study of 29 cases. Am. J. Surg. Pathol. *31*, 697–705.

Alimonti, A., Nardella, C., Chen, Z., Clohessy, J.G., Carracedo, A., Trotman, L.C., Cheng, K., Varmeh, S., Kozma, S.C., Thomas, G., et al. (2010). A novel type of cellular senescence that can be enhanced in mouse models and human tumor xenografts to suppress prostate tumorigenesis. J. Clin. Invest. *120*, 681–693.

Backman, S.A., Ghazarian, D., So, K., Sanchez, O., Wagner, K.U., Hennighausen, L., Suzuki, A., Tsao, M.S., Chapman, W.B., Stambolic, V., and Mak, T.W. (2004). Early onset of neoplasia in the prostate and skin of mice with tissue-specific deletion of Pten. Proc. Natl. Acad. Sci. USA *101*, 1725–1730.

Bonkhoff, H., Stein, U., and Remberger, K. (1994). The proliferative function of basal cells in the normal and hyperplastic human prostate. Prostate *24*, 114–118.

Burger, P.E., Xiong, X., Coetzee, S., Salm, S.N., Moscatelli, D., Goto, K., and Wilson, E.L. (2005). Sca-1 expression identifies stem cells in the proximal region of prostatic ducts with high capacity to reconstitute prostatic tissue. Proc. Natl. Acad. Sci. USA *102*, 7180–7185.

Chen, Z., Trotman, L.C., Shaffer, D., Lin, H.K., Dotan, Z.A., Niki, M., Koutcher, J.A., Scher, H.I., Ludwig, T., Gerald, W., et al. (2005). Crucial role of p53-dependent cellular senescence in suppression of Pten-deficient tumorigenesis. Nature *436*, 725–730.

Donjacour, A.A., Rosales, A., Higgins, S.J., and Cunha, G.R. (1990). Characterization of antibodies to androgen-dependent secretory proteins of the mouse dorsolateral prostate. Endocrinology *126*, 1343–1354.

Dor, Y., Brown, J., Martinez, O.I., and Melton, D.A. (2004). Adult pancreatic beta-cells are formed by self-duplication rather than stem-cell differentiation. Nature *429*, 41–46.

Ellwood-Yen, K., Graeber, T.G., Wongvipat, J., Iruela-Arispe, M.L., Zhang, J., Matusik, R., Thomas, G.V., and Sawyers, C.L. (2003). Myc-driven murine prostate cancer shares molecular features with human prostate tumors. Cancer Cell *4*, 223–238.

Foster, B.A., Gingrich, J.R., Kwon, E.D., Madias, C., and Greenberg, N.M. (1997). Characterization of prostatic epithelial cell lines derived from transgenic adenocarcinoma of the mouse prostate (TRAMP) model. Cancer Res. *57*, 3325–3330.

Goldstein, A.S., Huang, J., Guo, C., Garraway, I.P., and Witte, O.N. (2010). Identification of a cell of origin for human prostate cancer. Science *329*, 568–571.

Iczkowski, K.A., and Lucia, M.S. (2011). Current perspectives on Gleason grading of prostate cancer. Curr. Urol. Rep. *12*, 216–222.

Iwata, T., Schultz, D., Hicks, J., Hubbard, G.K., Mutton, L.N., Lotan, T.L., Bethel, C., Lotz, M.T., Yegnasubramanian, S., Nelson, W.G., et al. (2010). MYC overexpression induces prostatic intraepithelial neoplasia and loss of Nkx3.1 in mouse luminal epithelial cells. PLoS ONE *5*, e9427.

Jäämaa, S., Af Hällström, T.M., Sankila, A., Rantanen, V., Koistinen, H., Stenman, U.H., Zhang, Z., Yang, Z., De Marzo, A.M., Taari, K., et al. (2010). DNA damage recognition via activated ATM and p53 pathway in nonproliferating human prostate tissue. Cancer Res. *70*, 8630–8641.

Lawson, D.A., and Witte, O.N. (2007). Stem cells in prostate cancer initiation and progression. J. Clin. Invest. *117*, 2044–2050.

Lawson, D.A., Xin, L., Lukacs, R.U., Cheng, D., and Witte, O.N. (2007). Isolation and functional characterization of murine prostate stem cells. Proc. Natl. Acad. Sci. USA *104*, 181–186.

Lawson, D.A., Zong, Y., Memarzadeh, S., Xin, L., Huang, J., and Witte, O.N. (2010). Basal epithelial stem cells are efficient targets for prostate cancer initiation. Proc. Natl. Acad. Sci. USA *107*, 2610–2615.

Leong, K.G., Wang, B.E., Johnson, L., and Gao, W.Q. (2008). Generation of a prostate from a single adult stem cell. Nature *456*, 804–808.

Lim, E., Vaillant, F., Wu, D., Forrest, N.C., Pal, B., Hart, A.H., Asselin-Labat, M.L., Gyorki, D.E., Ward, T., Partanen, A., et al; kConFab. (2009). Aberrant luminal progenitors as the candidate target population for basal tumor development in BRCA1 mutation carriers. Nat. Med. *15*, 907–913.

Litvinov, I.V., Vander Griend, D.J., Xu, Y., Antony, L., Dalrymple, S.L., and Isaacs, J.T. (2006). Low-calcium serum-free defined medium selects for growth of normal prostatic epithelial stem cells. Cancer Res. *66*, 8598–8607.

Liu, J., Pascal, L.E., Isharwal, S., Metzger, D., Ramos Garcia, R., Pilch, J., Kasper, S., Williams, K., Basse, P.H., Nelson, J.B., et al. (2011). Regenerated luminal epithelial cells are derived from preexisting luminal epithelial cells in adult mouse prostate. Mol. Endocrinol. *25*, 1849–1857.

Majumder, P.K., Yeh, J.J., George, D.J., Febbo, P.G., Kum, J., Xue, Q., Bikoff, R., Ma, H., Kantoff, P.W., Golub, T.R., et al. (2003). Prostate intraepithelial neoplasia induced by prostate restricted Akt activation: the MPAKT model. Proc. Natl. Acad. Sci. USA *100*, 7841–7846.

Molyneux, G., Geyer, F.C., Magnay, F.A., McCarthy, A., Kendrick, H., Natrajan, R., Mackay, A., Grigoriadis, A., Tutt, A., Ashworth, A., et al. (2010). BRCA1 basal-like breast cancers originate from luminal epithelial progenitors and not from basal stem cells. Cell Stem Cell *7*, 403–417.

Mulholland, D.J., Xin, L., Morim, A., Lawson, D., Witte, O., and Wu, H. (2009). Lin-Sca-1+CD49fhigh stem/progenitors are tumor-initiating cells in the Pten-null prostate cancer model. Cancer Res. *69*, 8555–8562.

Muzumdar, M.D., Tasic, B., Miyamichi, K., Li, L., and Luo, L. (2007). A global double-fluorescent Cre reporter mouse. Genesis *45*, 593–605.

Neubauer, B.L., Chung, L.W., McCormick, K.A., Taguchi, O., Thompson, T.C., and Cunha, G.R. (1983). Epithelial-mesenchymal interactions in prostatic development. II. Biochemical observations of prostatic induction by urogenital sinus mesenchyme in epithelium of the adult rodent urinary bladder. J. Cell Biol. *96*, 1671–1676.

Park, J.H., Walls, J.E., Galvez, J.J., Kim, M., Abate-Shen, C., Shen, M.M., and Cardiff, R.D. (2002). Prostatic intraepithelial neoplasia in genetically engineered mice. Am. J. Pathol. *161*, 727–735.

Peehl, D.M. (2005). Primary cell cultures as models of prostate cancer development. Endocr. Relat. Cancer *12*, 19–47.

Ratnacaram, C.K., Teletin, M., Jiang, M., Meng, X., Chambon, P., and Metzger, D. (2008). Temporally controlled ablation of PTEN in adult mouse prostate epithelium generates a model of invasive prostatic adenocarcinoma. Proc. Natl. Acad. Sci. USA *105*, 2521–2526.

Taylor, R.A., Cowin, P.A., Cunha, G.R., Pera, M., Trounson, A.O., Pedersen, J., and Risbridger, G.P. (2006). Formation of human prostate tissue from embryonic stem cells. Nat. Methods *3*, 179–181.

Tsujimura, A., Koikawa, Y., Salm, S., Takao, T., Coetzee, S., Moscatelli, D., Shapiro, E., Lepor, H., Sun, T.T., and Wilson, E.L. (2002). Proximal location of mouse prostate epithelial stem cells: a model of prostatic homeostasis. J. Cell Biol. *157*, 1257–1265.

Tuxhorn, J.A., Ayala, G.E., and Rowley, D.R. (2001). Reactive stroma in prostate cancer progression. J. Urol. *166*, 2472–2483.

Van Keymeulen, A., Rocha, A.S., Ousset, M., Beck, B., Bouvencourt, G., Rock, J., Sharma, N., Dekoninck, S., and Blanpain, C. (2011). Distinct stem cells contribute to mammary gland development and maintenance. Nature *479*, 189–193.

Vasioukhin, V., Degenstein, L., Wise, B., and Fuchs, E. (1999). The magical touch: genome targeting in epidermal stem cells induced by tamoxifen application to mouse skin. Proc. Natl. Acad. Sci. USA *96*, 8551–8556.

Visvader, J.E. (2011). Cells of origin in cancer. Nature *469*, 314–322.

Wang, S., Gao, J., Lei, Q., Rozengurt, N., Pritchard, C., Jiao, J., Thomas, G.V., Li, G., Roy-Burman, P., Nelson, P.S., et al. (2003). Prostate-specific deletion of the murine Pten tumor suppressor gene leads to metastatic prostate cancer. Cancer Cell *4*, 209–221.

Wang, S., Garcia, A.J., Wu, M., Lawson, D.A., Witte, O.N., and Wu, H. (2006). Pten deletion leads to the expansion of a prostatic stem/progenitor cell subpopulation and tumor initiation. Proc. Natl. Acad. Sci. USA *103*, 1480–1485.

Wang, X., Kruithof-de Julio, M., Economides, K.D., Walker, D., Yu, H., Halili, M.V., Hu, Y.P., Price, S.M., Abate-Shen, C., and Shen, M.M. (2009). A luminal epithelial stem cell that is a cell of origin for prostate cancer. Nature *461*, 495–500.

Wang, Y., Hayward, S., Cao, M., Thayer, K., and Cunha, G. (2001). Cell differentiation lineage in the prostate. Differentiation *68*, 270–279.

Wu, C.T., Altuwaijri, S., Ricke, W.A., Huang, S.P., Yeh, S., Zhang, C., Niu, Y., Tsai, M.Y., and Chang, C. (2007). Increased prostate cell proliferation and loss of cell differentiation in mice lacking prostate epithelial androgen receptor. Proc. Natl. Acad. Sci. USA *104*, 12679–12684.

Xin, L., Ide, H., Kim, Y., Dubey, P., and Witte, O.N. (2003). In vivo regeneration of murine prostate from dissociated cell populations of postnatal epithelia and urogenital sinus mesenchyme. Proc. Natl. Acad. Sci. USA *100* (*Suppl 1*), 11896–11903.

Xin, L., Lawson, D.A., and Witte, O.N. (2005). The Sca-1 cell surface marker enriches for a prostate-regenerating cell subpopulation that can initiate prostate tumorigenesis. Proc. Natl. Acad. Sci. USA *102*, 6942–6947.

Xin, L., Lukacs, R.U., Lawson, D.A., Cheng, D., and Witte, O.N. (2007). Self-renewal and multilineage differentiation in vitro from murine prostate stem cells. Stem Cells *25*, 2760–2769.

Yao, D., Alexander, C.L., Quinn, J.A., Porter, M.J., Wu, H., and Greenhalgh, D.A. (2006). PTEN loss promotes rasHa-mediated papillomatogenesis via dual up-regulation of AKT activity and cell cycle deregulation but malignant conversion proceeds via PTEN-associated pathways. Cancer Res. *66*, 1302–1312.

Zhang, L., Valdez, J.M., Zhang, B., Wei, L., Chang, J., and Xin, L. (2011). ROCK inhibitor Y-27632 suppresses dissociation-induced apoptosis of murine prostate stem/progenitor cells and increases their cloning efficiency. PLoS ONE *6*, e18271.

Zhang, L., Zhang, B., Han, S.J., Shore, A.M, Rosen, J.M., DeMayo, F.J., and Xin, L. (2012). Targeting CreERT2 expression to Keratin 8-expressing murine simple epithelia using bacterial artificial chromosome transgenesis. Transgenic Research, in press.